Melatonin Attenuates LPS-Induced Proinflammatory Cytokine Response and Lipogenesis in Human Meibomian Gland Epithelial Cells via MAPK/NF-κB Pathway

Ren Liu, Jing Li, Yue Xu, Ziyan Chen, Huijing Ye, Jinhui Tang, Lai Wei, and Lingyi Liang

State Key Laboratory of Ophthalmology, Zhongshan Ophthalmic Center, Sun Yat-sen University, Guangdong Provincial Key Laboratory of Ophthalmology and Visual Science, Guangzhou, China

Correspondence: Lingyi Liang, Zhongshan Ophthalmic Center, 54S Xianlie Nan Road, Guangzhou 510060, China; lianglingyi@gzzoc.com.

Received: January 18, 2022
Accepted: April 16, 2022
Published: May 4, 2022

Citation: Liu R, Li J, Xu Y, et al. Melatonin attenuates LPS-induced proinflammatory cytokine response and lipogenesis in human meibomian gland epithelial cells via MAPK/NF-κB pathway. *Invest Ophthalmol Vis Sci.* 2022;63(5):6. https://doi.org/10.1167/iovs.63.5.6

Purpose. Inflammation contributes to the development of meibomian gland dysfunction (MGD) under specific disease conditions, but the underlying mechanisms remain elusive. We examined whether lipopolysaccharide (LPS) induced a proinflammatory cytokine response and lipogenesis in human meibomian gland epithelial cells (HMGECs) and whether melatonin (MLT), a powerful anti-inflammatory regent in the eyes, could protect against LPS-induced disorders.

Methods. Human meibomian gland (MG) tissues and immortalized HMGECs were stained to identify Toll-like receptor (TLR) 4 and MLT receptors (MT_1 and MT_2). HMGECs were pretreated with or without MLT and then stimulated with LPS. Then, TLR4 activation, cytokine levels, lipid synthesis, apoptosis, autophagy, and MAPK/NF-κB factor phosphorylation in HMGECs were analyzed.

Results. TLR4, MT_1, and MT_2 were expressed in human MG acini and HMGECs. Pretreatment with MLT inhibited the TLR4/MyD88 signaling and attenuated proinflammatory cytokine response and lipogenesis in LPS-stimulated HMGECs, which manifested as decreased production of cytokines (IL-1β, IL-6, IL-8, and TNF-α), reduced lipid droplet formation, and downregulated expression of meibum lipogenic proteins (ADFP, ELOVL4, and SREBP-1). Phospho-histone H2A.X foci, lysosome accumulation, and cytoplasmic cleaved caspase 3/LC3B-II staining were increased in LPS-stimulated HMGECs, indicating enhanced cell death mediated by apoptosis and autophagy during LPS-induced lipogenesis. MLT downregulated cleaved caspase 3 levels and the Bax/Bcl-2 ratio to alleviate apoptosis and ameliorated the expression of Beclin 1 and LC3B-II to inhibit autophagy. The protective mechanisms of MLT include the inhibition of MAPK and NF-κB phosphorylation.

Conclusions. MLT attenuated lipogenesis, apoptosis, and autophagy in HMGECs induced by proinflammatory stimuli, indicating the protective potential of MLT in MGD.

Keywords: melatonin, meibomian gland, TLR4, proinflammatory cytokine response, lipogenesis

The meibomian gland (MG) is the largest sebaceous gland (SG) in humans and is composed of three types of epithelial cells: progenitor, differentiated, and ductal cells.[1] The MG produces meibum through holocrine secretion. Briefly, differentiated meibocytes pack lipids into the ductal system in the presence of DNA degradation and cytoplasmic rupture; then, the meibum is subsequently released to the ocular surface, and the meibocytes eventually die.[2] Human meibomian gland epithelial cells (HMGECs) can differentiate into meibocytes and produce lipids in vitro.[3] The qualitative or quantitative changes in the lipid profiles of the meibum induce MG ductal obstruction or glandular dropout, which is also called meibomian gland dysfunction (MGD).[1] MGD destroys tear film structure and increases tearing osmolarity, contributing to evaporative dry eye disease.[4] The worldwide prevalence of MGD is as high as 36.8%,[5] and it has become a widespread eye disease affecting quality of life,[6] but the pathologic mechanisms of MGD remain unclear.

According to the classical consensus of MGD pathophysiology, inflammation is not considered a characteristic component of MGD development.[1,7] However, recent studies have provided evidence that inflammation could contribute to MGD under specific disease conditions.[8–11] A significant correlation between neutrophil influx and MG occlusion was found in patients with chronic blepharitis, chalazion, and trichiasis.[9] In addition, prominent inflammatory cell infiltration and proinflammatory cytokine responses were detected in the MG microenvironment in a rodent MGD model induced by hyperlipidemia and hyperglycemia.[10,11] Abnormal accumulation of intraductal lipids from meibocytes and hyperkeratinization of MG ductal cells are important features of MGD.[8,12] Studies have reported that the pathology of ductal hyperkeratinization involves the overexpression of keratin 1 in MG ductal cells induced by proinflammatory stimulation.[13,14] In the SG, extracellular administration of *Propionibacterium acnes* and palmitic acid can

Copyright 2022 The Authors

This work is licensed under a Creative Commons Attribution-NonCommercial-NoDerivatives 4.0 International License.

Downloaded from hwmaint.iovs.org on 04/19/2024

trigger a proinflammatory cytokine response and lipogenesis in sebocytes.[15,16] However, relevant knowledge of human meibocytes is still insufficient.

Melatonin (MLT), a neurohormone that was first identified in the pineal gland,[17] is an indoleamine involved in various physiologic processes, among which most are associated with the control of circadian rhythms.[18] MLT activates specific receptors to mediate downstream actions. Two MLT receptors, MLT receptor 1 (MT_1) and MLT receptor 2 (MT_2), have been identified and cloned in humans, both of which belong to the seven-transmembrane G protein–coupled receptor family[19,20] and are widely distributed in ocular tissues.[21,22] The ability to synthesize and release MLT is not unique to the pineal gland. MLT has been detected in several eye areas, including the retina,[23] lens,[24] iris/ciliary body,[25] and lacrimal gland,[26] and there are effective concentrations within tears and aqueous humor.[27,28] MLT has exerted strong anti-inflammatory effects on the eyes, and pretreatment has significantly prevented bacterial lipopolysaccharide (LPS)–induced experimental uveitis and optic neuritis.[29,30] Notably, MLT also exhibits potent lipid regulatory effects on a variety of lipogenic cells,[31,32] further indicating that MLT may have regulatory effects on the MG. Therefore, identifying MLT receptors in human MG and further exploring the protective effects of MLT on MG are necessary.

Herein, we first identified MLT receptors in human meibocytes. We tested our hypothesis by investigating the effects of MLT on the proinflammatory cytokine response and lipogenesis induced by LPS in HMGECs. Information garnered from this study may provide insight into the pathology of MGD and has implications for understanding the anti-inflammatory role of MLT on the ocular surface.

Materials and Methods

Human Tissues

Human MG tissues were obtained within 2 hours after traumatic cicatricial ectropion/entropion surgeries: a 26-year-old man, a 51-year-old woman, and a 50-year-old woman. Patients with any previous other eye diseases except mild myopia in both eyes had been excluded. The use of human tissues conformed to the provisions of the Declaration of Helsinki and was approved by the Institutional Review Board of the Sun Yat-Sen University Zhongshan Ophthalmic Center (No. 2021KYPJ165). All surgical participants received a complete explanation of the study, and written informed consent was obtained.

Immunohistochemical Staining

Human MG tissues were fixed with 4% paraformaldehyde and subsequently embedded in paraffin after a series of sucrose gradients (10%, 20%, 30%). Tissue sections (6 µm) were briefly deparaffinized in xylene solution and rehydrated in a decreased alcohol series. For antigen retrieval of immunostaining, tissue slides were incubated in 10 mM sodium citrate buffer at 80°C for 10 minutes and cooled until room temperature, and slides were then treated with 3% hydrogen peroxide to block endogenous peroxidase activity. Tissue slides were blocked with phosphate-buffered saline plus 0.1% Tween-20 (PBST) containing 10% donkey serum and then incubated overnight with primary rabbit antibodies: Toll-like receptor (TLR) 4 (1:150; #29072; Signalway Antibody, Nanjing, China), MT_1 (1:100, ab203038; Abcam, Cambridge, MA, USA), and MT_2 (1:100, ab203346; Abcam). Tissue slides were washed with PBS, followed incubation with horseradish peroxidase–conjugated secondary antibody (1:1000, ab6802; Abcam). All tissue samples were captured by Tissue FAXS Q+ (TissueGnostics, Vienna, Austria).

Cell Culture

Authenticated immortalized HMGECs (a generous gift from David Sullivan, Schepens Eye Research Institute, Boston, MA, USA) were cultured in keratinocyte serum-free medium (KSFM; Invitrogen-Gibco, Grand Island, NY, USA) supplemented with epidermal growth factor (EGF, 5 ng/mL; Invitrogen-Gibco) and bovine pituitary extract (50 µg/mL; Absin, Shanghai, China) as previously described.[3] At 80% confluency, the cell medium was changed by Dulbecco's modified Eagle's medium and Ham's F12 (DMEM-F12; Invitrogen-Gibco) supplemented with EGF (10 ng/mL) and 10% fetal bovine serum (Invitrogen-Gibco) for cellular differentiation. The HMGECs pretreated with MLT (Sigma-Aldrich, St. Louis, MO, USA) or isochoric dimethyl sulfoxide (DMSO; Sigma-Aldrich) for 48 hours were characterized as the MLT group and the control group, respectively, while those that subsequently received 10 µg/mL LPS (*Escherichia coli*, strain 0127:B8, Sigma-Aldrich) were defined as LPS + MLT group and LPS group, respectively. The dose of LPS was used as previously described.[33]

Cell Viability Assay and Growth Curve

Cell viability and growth curve were both performed via the Cell Counting Kit-8 assay (CCK8; Dojindo, Kumamoto, Japan). HMGECs were seeded in 96-well plates at a density of 5×10^3 cells/well for 12 hours at KFSM. For assessing cell viability, cells were further treated with MLT ranging from 10 µM to 2 mM for 48 hours. For evaluating cell growth, day 0 was defined as 12 hours after cell seeding, and then cells were treated with MLT for another 24 and 48 hours, a column with the cell-free medium was set as background control. Then, 10 µL CCK8 solution per well was added and incubated at 37°C for another 4 hours. The optical density (OD) value was measured at 450 nm using a microplate reader (BioTek Instruments, Inc., Winooski, VT, USA).

ELISA Assay

ELISA was performed according to the manufacturer's instructions (RayBiotech, Norcross, GA, USA). Briefly, the HMGECs were seeded in 6-well plates at a density of 1×10^5/well until 80% confluency and then received indicated treatments. Cell supernatants were collected to analyze the level of proinflammatory cytokines (IL-1β, IL-6, IL-8, and TNF-α). The OD value was measured at 450 nm by the microplate reader.

Lipid and Lysosome Analysis

HMGECs were seeded in 24-well plates at a density of 2×10^4 cells/well until 80% confluency, and differentiation was then induced by MLT and LPS. For lipid analysis, cell slides were first fixed with 4% paraformaldehyde for 25 minutes at 4°C and then exposed to the neutral lipid droplet with HCS LipidTox solution (1:500;

Investigative Ophthalmology & Visual Science

Downloaded from hwmaint.iovs.org on 04/19/2024

Invitrogen-Gibco) for 30 minutes. For lysosome staining, cells were further stained in a medium containing LysoTracker Deep Red (1:20,000; Invitrogen-Gibco) for 30 minutes. Slides were counterstained with 4′,6-diamidino-2-phenylindole (DAPI, 1 µg/mL; Biofroxx, Einhausen, Germany) for 15 minutes to allow nuclei visualization. Cell slides were observed and captured under the confocal laser scanning microscope (LSM 980; Zeiss, Oberkochen, Germany), and fluorescence intensities were quantified with ImageJ (National Institutes of Health, Bethesda, MD, USA).

Immunofluorescence Staining

HMGECs for staining were seeded in 24-well plates at a density of 2×10^4 cells/well. Cell slides were fixed with 4% paraformaldehyde and permeabilized using 0.2% Triton X-100. Cell slides were further blocked with PBS containing 3% BSA (Sigma-Aldrich) and then incubated with the primary antibodies, including TLR4 (1:150, #29072; Signalway Antibody), MT_1 (1:150, SC-390328; Santa Cruz Biotechnology, Santa Cruz, CA, USA), MT_2 (1:150, ab203346; Abcam), phospho-histone H2A.X (1:400, #9718; Cell Signaling Technology, Boston, MA, USA), and cleaved caspase 3 (1:400, #9661; Cell Signaling Technology, Boston, MA, USA) overnight. The samples were subsequently incubated with fluorescein-conjugated secondary antibody: Alexa Fluor 488– or Alexa Fluor 555–labeled donkey anti-rabbit IgG antibody (1:1000, 488-ab150073, 555-ab155062; Abcam) and Alexa Fluor 555–labeled donkey anti-mouse IgG antibody (1:1000, ab150110; Abcam). All staining was further incubated with DAPI and captured under a confocal laser scanning microscope (LSM 980; Zeiss).

Quantitative Real-Time Polymerase Chain Reaction

HMGECs for mRNA extraction were seeded in 12-well plates at a density of 5×10^4 cells/well. mRNA expression of TLR4, IL-1β, IL-6, IL-8, TNF-α, IL-12, IFN-γ, MMP-3, and MMP-9 (Table) was evaluated through quantitative RT-PCR (qRT-PCR). RNA was isolated using the FastPure Cell Total RNA Isolation Kit V2 (Vazyme, Nanjing, China) and qualified and quantified with Nanodrop (Thermo Scientific, Waltham, MA, USA). Then, 500 ng RNA was reverse transcribed with oligo dT and random primers as provided in the HiScript II Transcription Kit (Vazyme). qRT-PCR was performed with the SYBR green mix via the Lightcycler 96 system (LC96; Roche, Mannheim, Germany). The relative quantities of gene expressions were analyzed by using the comparative $2^{-\Delta\Delta Ct}$ method, and glyceraldehyde-3-phosphate dehydrogenase was characterized as the normalizing housekeeper gene.

Protein Extraction and Western Blot

HMGECs for protein extraction were seeded in 6-well plates at a density of 1×10^5 cells/well. After indicated treatment, HMGECs were harvested for protein extraction by RIPA lysis buffer containing phenylmethylsulfonyl fluoride and phosphatase inhibitor cocktail (all purchased from Sigma-Aldrich). Cellular protein was quantified by a protein quantification kit (Solarbio, Beijing, China) via spectrophotometer at 562 nm, and then a reducing buffer containing β-mercaptoethanol was added to boil protein. In total, 25 µg protein was loaded into a 10% to 12% SDS-PAGE gel and electrophoretically transferred to a nitrocellulose membrane through the electroblotting system (all bought from Bio-Rad, Hercules, CA, USA). Primary antibodies were diluted in tris-buffered saline with tween-20 (TBST) with 3% BSA to incubate the membrane at 4°C overnight (Supplementary Table S1). Following additional washing, the membrane was further incubated with horseradish peroxidase–conjugated secondary antibody (1:5000, ab6802, ab6378; Abcam). Each target protein of the antibodies was visualized using enhanced chemiluminescence reagents and recorded by the Bio-Rad Gel Doc XR Gel Documentation System. All results were analyzed through Image Lab 5.1 software (Bio-Rad).

Statistical Analysis

Unpaired two-tailed Student's *t*-tests and one-way ANOVA were used to determine statistical significance for all experimental data via SPSS software (version 19.0; SPSS, Inc., Chicago, IL, USA). Data are presented as mean ± SEM at the confidence level of $P < 0.05$. All experiments were repeated at least three times to ensure credibility.

Results

LPS Triggered a TLR4-Mediated Proinflammatory Cytokine Response in HMGECs

We first carried out immunostaining to identify the expression of the LPS sensor TLR4 in human MG and HMGECs. As shown in Figure 1A, TLR4 was distributed in the acini of human MG and was nearly undetectable in the negative control. Immunofluorescence staining also showed that TLR4 was diffusely distributed in the cytoplasm of

Table. Primers Used for qRT-PCR in This Study

Gene	Forward (5′-3′)	Reverse (3′-5′)	Product Length, bp
GAPDH	TCCAAAATCAAGTGGGGCGA	TGATGACCCTTTTGGCTCCC	115
TLR4	TGCGTGGAGGTGGTTCCTAA	GCCTAAATGCCTCAGGGGAT	126
IL-1β	CAGAAGTACCTGAGCTCGCC	AGATTCGTAGCTGGATGCCG	153
IL-6	CCAGTACCCCCAGGAGAAGA	TGTTTTCTGCCAGTGCCTCT	181
IL-8	ACTCCAAACCTTTCCACCCC	ATGAATTCTCAGCCCTCTTCAA	180
TNF-α	GCCCATGTTGTAGCAAACCC	GAGGTACAGGCCCTCTGATG	132
IL-12	TTTTCTGGCATCTCCCCTCG	GCCAGAGCCTAAGACCTCAC	175
IFN-γ	ACCAGAGCATCCAAAAGAGTGT	TTAGCTGCTGGCGACAGTTC	187
MMP-3	TGGGCCAGGGATTAATGGAG	GGAACCGAGTCAGGTCTGTG	188
MMP-9	TTTGAGTCCGGTGGACGATG	GCTCCTCAAAGACCGAGTCC	197

GAPDH, glyceraldehyde-3-phosphate dehydrogenase.

Investigative Ophthalmology & Visual Science

Downloaded from hwmaint.iovs.org on 04/19/2024

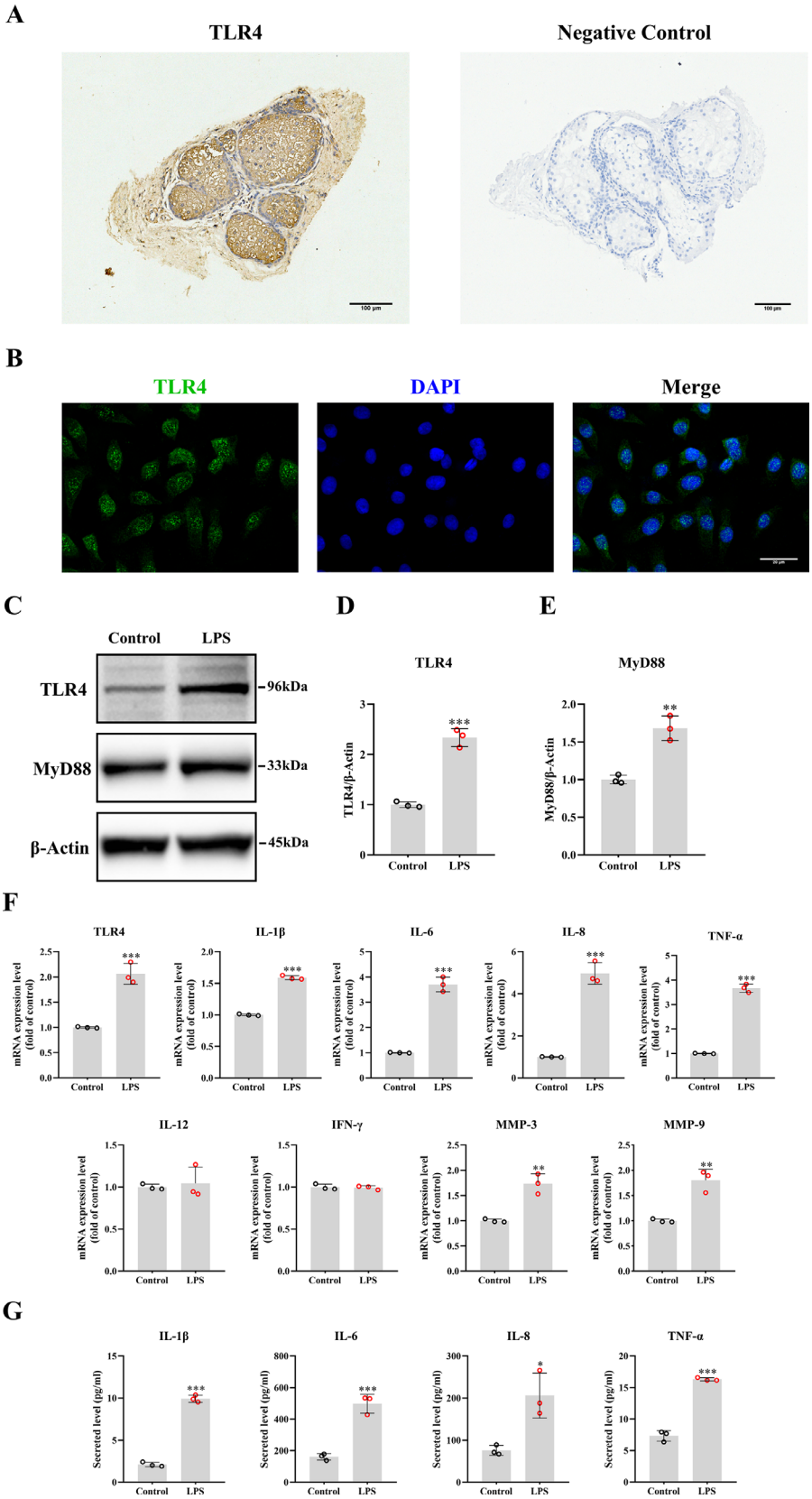

Figure 1. Effects of LPS on TLR4-mediated proinflammatory cytokine response in differentiated HMGECs. (**A**) Expression of TLR4 in human MG specimens detected by immunohistochemical staining. *Scale bar*: 100 µm. (**B**) Expression of TLR4 in HMGECs depicted by immunofluorescence staining. *Scale bar*: 20 µm. The HMGECs were treated with differentiated medium for 48 hours followed by LPS (10 µg/mL) for 8 hours. (**C**) Representative protein bands of TLR4 and MyD88. (**D**, **E**) Quantitative intensity of TLR4 and MyD88. (**F**) Transcriptional levels of TLR4 and cytokines. (**G**) Secreted levels of cytokines. $n = 3$. *Significantly different from control, $^{*}P < 0.05$, $^{**}P < 0.01$, $^{***}P < 0.001$. MyD88, myeloid differentiation factor.

Investigative Ophthalmology & Visual Science

Downloaded from hwmaint.iovs.org on 04/19/2024

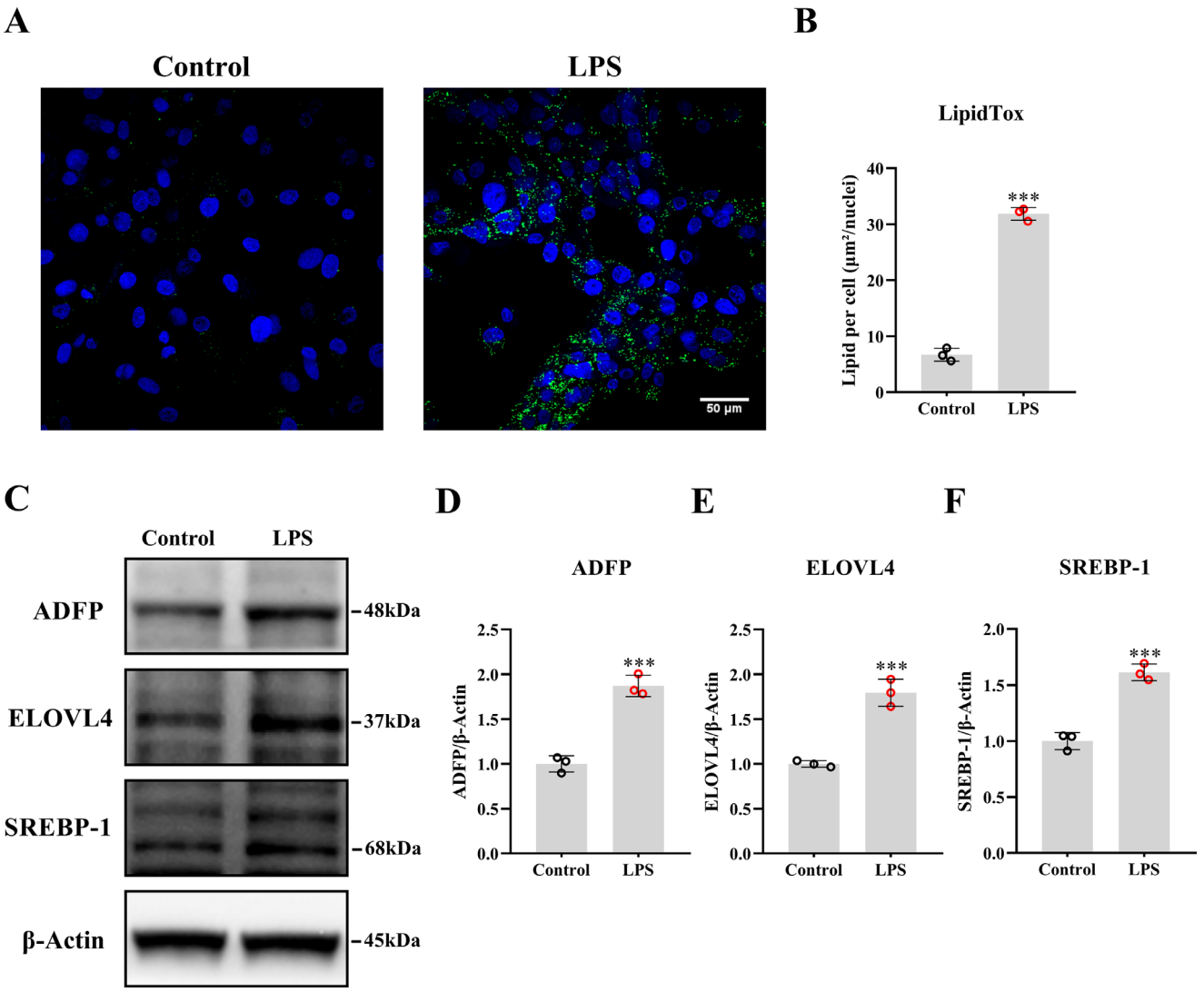

Figure 2. Effects of LPS on lipogenesis in differentiated HMGECs. The HMGECs were exposed to differentiated medium for 48 hours followed by LPS for 24 hours. (**A**) Images of lipid droplets in HMGECs detected by LipidTox staining. *Scale bar*: 50 μm. (**B**) Densitometric analysis and quantification of lipid droplets. (**C**) Representative protein bands of ADFP, ELOVL4, and SREBP-1. (**D–F**) Relative intensity of ADFP (**D**), ELOVL4 (**E**), and SREBP-1 (**F**). $n = 3$. ***Significantly different from control, $P < 0.001$.

HMGECs (Fig. 1B). Treatment of HMGECs with 10 μg/mL LPS significantly activated TLR4 signaling by upregulating the protein expression of TLR4 and MyD88 compared with those in the control (Figs. 1C–E). Compared with the control group, LPS markedly promoted the transcription of TLR4 (2.0-fold) and upregulated the mRNA levels of proinflammatory cytokine IL-1β (1.6-fold), IL-6 (3.7-fold), IL-8 (4.9-fold), and TNF-α (3.6-fold) and the matrix-degrading cytokines MMP-3 (1.7-fold) and MMP-9 (1.8-fold) in HMGECs (all $P < 0.05$, Fig. 1F). Similarly, the secretion of proinflammatory cytokines was upregulated after LPS stimulation, as determined by ELISA measurements (all $P < 0.05$, Fig. 1G). However, LPS showed no effects on the mRNA levels of IL-12 and IFN-γ.

Proinflammatory Stimuli Induced Lipogenesis in HMGECs

The results of LipidTox staining depicted that the number of lipid droplets was prominently increased in the LPS-stimulated group compared with the control group (Figs. 2A, 2B, $P < 0.001$). Adipose differentiation-related protein (ADFP) expression in the LPS group was upregulated by 1.9-fold compared with that in the control group, indicating the stimulation of HMGEC differentiation (Figs. 2C, 2D). In addition, meibum lipogenic proteins, including elongation of very long-chain fatty acid protein 4 (ELOVL4) and sterol regulatory element-binding protein 1 (SREBP-1), were significantly upregulated after treatment with LPS by 1.8- and 1.6-fold, respectively (Figs. 2E, 2F). These results suggest that the LPS-evoked proinflammatory cytokine response may enhance lipogenesis in HMGECs.

MLT Receptor Identification and Concentration Selection

To address the possible role of MLT signaling in the MG, we first performed immunohistochemical analysis to examine the presence of MLT receptors in human eyelid samples. As shown in Figure 3A, both MT_1 and MT_2 were identified in the central acini of the MG. Immunofluorescence analysis of HMGECs also showed that MT_1 was mainly expressed in the

Investigative Ophthalmology & Visual Science

Downloaded from hwmaint.iovs.org on 04/19/2024

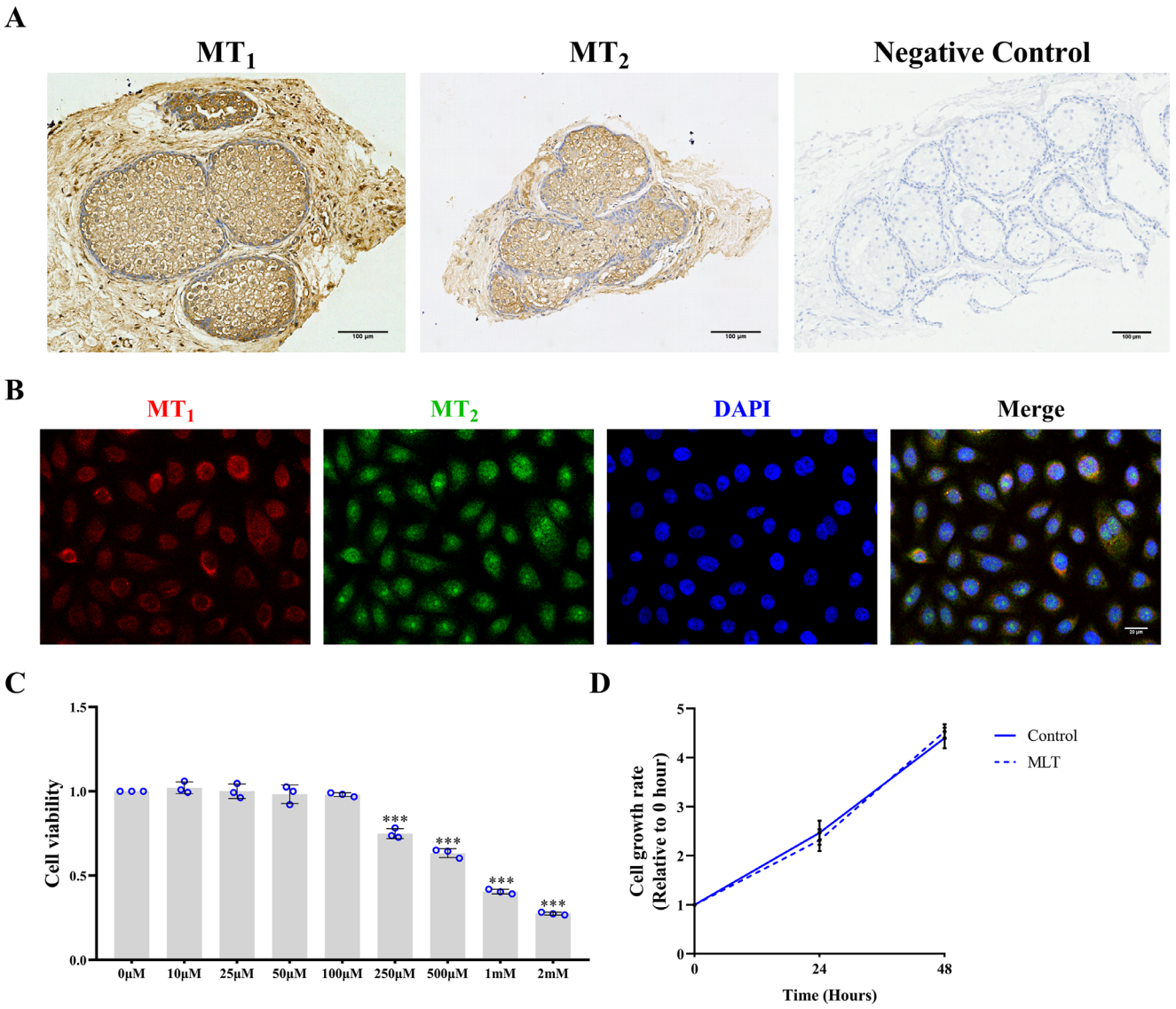

Figure 3. MLT receptors in human meibocytes and MLT concentration selection. (**A**) Expression of MT_1 and MT_2 in human MG specimens detected by immunohistochemical staining. *Scale bar*: 100 µm. (**B**) Expression of MT_1 and MT_2 in HMGECs depicted by immunofluorescence staining. *Scale bar*: 20 µm. (**C**) The HMGECs received MLT in a concentration-dependent manner for 48 hours to evaluate cell viability. (**D**) The HMGECs incubated with 100 µM MLT to 48 hours to assess cell growth rate ($n = 3$). ***Significantly different from control, $P < 0.001$.

cellular membrane, while MT_2 was widely expressed in the entire cell (Fig. 3B). We then selected the optimal concentration of MLT from 10 µM to 2 mM via CCK8 assays. High-dose MLT treatment for 48 hours decreased cellular viability in a dose-dependent manner (≥250 µM), but low doses (10–100 µM) did not affect HMGECs (Fig. 3C). MLT (100 µM) also failed to affect cell growth at 24 and 48 hours (Fig. 3D) and approached the physiologic concentration in tears[27]; therefore, 100 µM was used for the subsequent experiments.

Pretreatment With MLT Suppressed LPS-Induced Proinflammatory Cytokine Response and Lipogenesis

Pretreatment with MLT exerted notable anti-inflammatory effects on several inflammatory ocular diseases[29,30]; therefore, in the present study, we examined whether MLT could attenuate inflammatory cascades in LPS-stimulated HMGECs. As shown in Figures 4A–C, the protein levels of TLR4 (fold change: 2.2 vs. 1.5, $P < 0.001$) and MyD88 (fold change: 1.6 vs. 1.1, $P < 0.001$) were inhibited in MLT-treated HMGECs. MLT significantly suppressed LPS-induced transcriptional activation of TLR4 and downregulated the mRNA levels of IL-1β, IL-6, IL-8, TNF-α, MMP-3, and MMP-9 (Fig. 4D). Similarly, MLT significantly inhibited IL-1β, IL-6, IL-8, and TNF-α secretion (Fig. 4E).

We then performed LipidTox staining to evaluate the effects of MLT on LPS-induced lipogenesis. As expected, MLT significantly inhibited the LPS-induced accumulation of lipid droplets but did not induce extra lipogenesis in HMGECs (Figs. 5A, 5B, $P < 0.01$). MLT abrogated the LPS-induced upregulation of ADFP, ELOVL4, and SREBP-1 expression but exhibited no significant effect on basal expression (Figs. 5C–F).

Investigative Ophthalmology & Visual Science

Downloaded from hwmaint.iovs.org on 04/19/2024

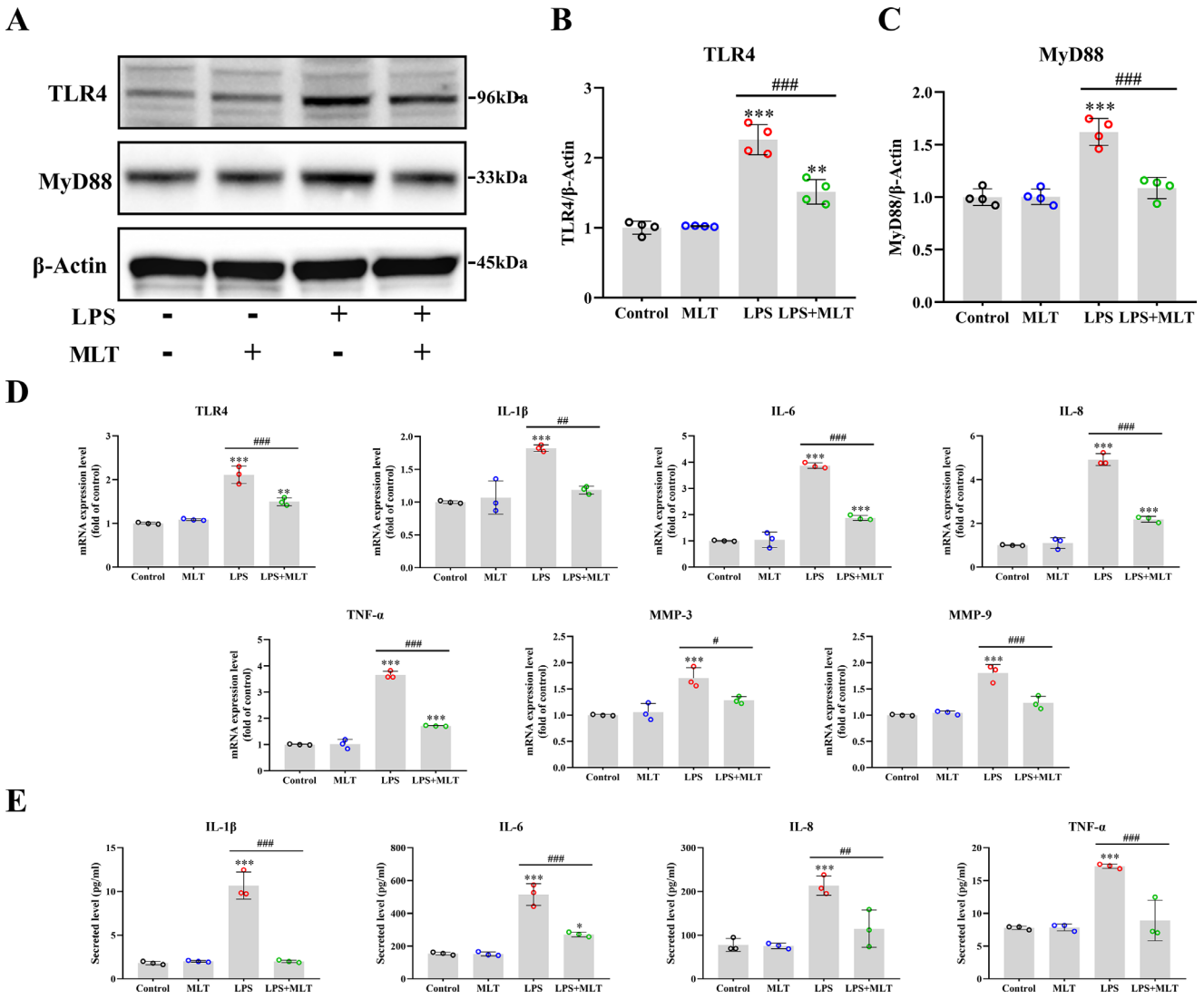

Figure 4. MLT inhibited TLR4-mediated proinflammatory cytokine response in LPS-stimulated HMGECs. The HMGECs were treated with MLT (100 μM) for 48 hours followed by LPS for 8 hours. (**A**) Representative protein bands of TLR4 and MyD88. (**B**, **C**) Quantitative intensity of TLR4 and MyD88 ($n = 4$). (**D**) Transcriptional levels of TLR4 and cytokines ($n = 3$). (**E**) Secreted levels of cytokines ($n = 3$). *Significantly different from control, $^{*}P < 0.05$, $^{**}P < 0.01$, $^{***}P < 0.001$. $^{\#}$Significantly different from LPS group, $^{\#}P < 0.05$, $^{\#\#}P < 0.01$, $^{\#\#\#}P < 0.001$.

Pretreatment With MLT Suppressed Lipogenesis-Related DNA Damage and Apoptosis in HMGECs

Programmed cell death contributes to the terminal differentiation of holocrine gland cells.[34] The immunofluorescence showed that phospho-histone H2A.X foci were observed in the differentiating HMGECs and were especially prominent in LPS-stimulated HMGECs compared with undifferentiated cells (Fig. 6A), indicating active strand breaks during HMGEC lipogenesis. In addition, there was a clear decrease in the labeling rate and protein expression (fold change: 2.3 vs. 1.5, $P < 0.001$) of phospho-histone H2A.X after pretreatment with MLT (Figs. 6A–C), suggesting a protective effect of MLT on LPS-induced DNA damage.

We then examined apoptosis in HMGECs. Immunofluorescence analysis of cleaved caspase 3 showed that cells in the LPS group exhibited more lipid droplets accompanied by prominent staining of cytoplasmic cleaved caspase 3 compared with that in the control (Figs. 6D–E, $P < 0.01$). Pretreatment with MLT significantly attenuated LPS-induced staining of cytoplasmic cleaved caspase 3. Western blotting showed consistent results: MLT inhibited LPS-induced caspase 3 cleavage (fold change: 2.5 vs. 1.6, $P < 0.001$, Figs. 6F, 6G) and significantly decreased the Bax/Bcl-2 ratio (fold change: 3.4 vs. 2.2, $P < 0.001$, Fig. 6H). These results suggest that MLT may inhibit LPS-induced lipogenesis-related DNA damage and apoptosis in HMGECs.

Pretreatment With MLT Suppressed LPS-Induced Lysosome Accumulation and Autophagy

During autophagy, toxic cytoplasmic contents trigger lysosome recruitment, which then facilitates the formation of autophagosomes.[35] In this study, we observed that

Investigative Ophthalmology & Visual Science

Downloaded from hwmaint.iovs.org on 04/19/2024

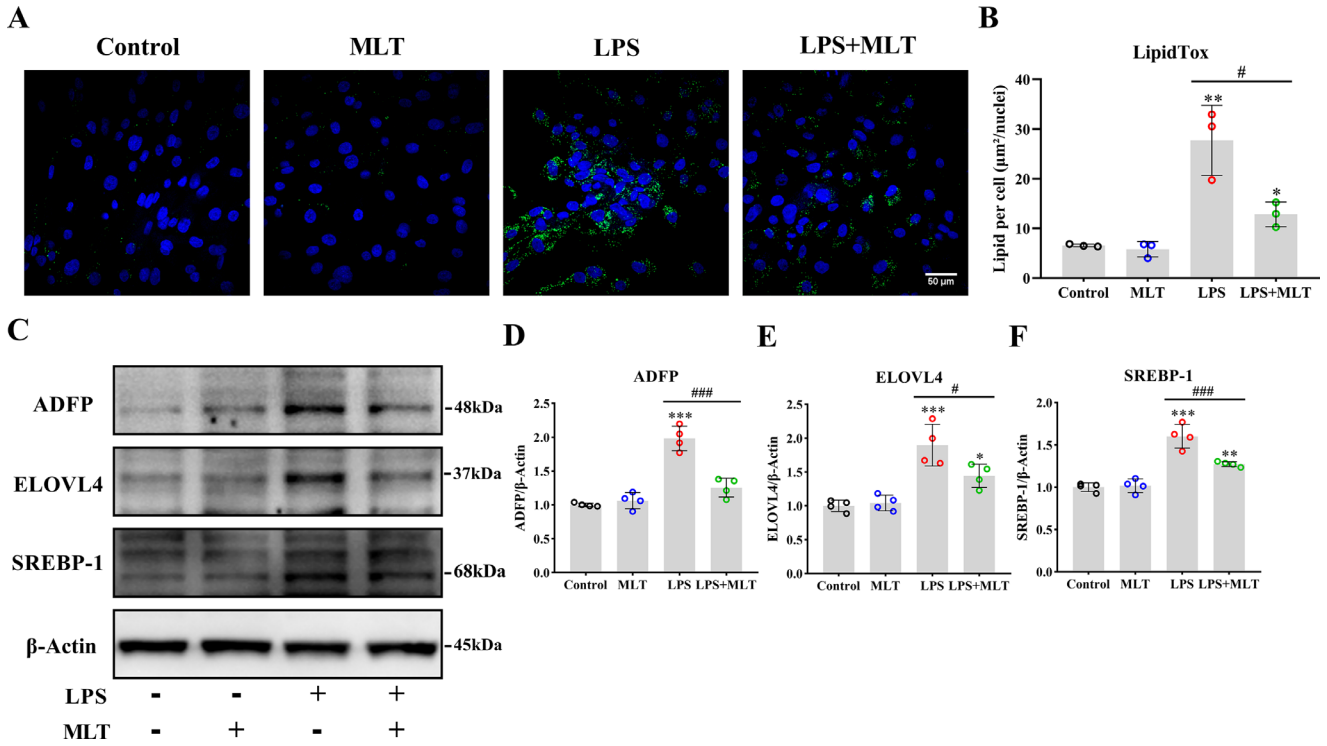

Figure 5. MLT attenuated lipogenesis in LPS-stimulated HMGECs. The HMGECs were treated with MLT for 48 hours followed by LPS for 24 hours. (**A**) Images of lipid droplets in HMGECs detected by LipidTox staining. *Scale bar*: 50 µm. (**B**) Densitometric analysis and quantification of lipid droplets ($n = 3$). (**C**) Representative protein bands of ADFP, ELOVL4, and SREBP-1. (**D–F**) Relative intensity of ADFP (**D**), ELOVL4 (**E**), and SREBP-1 (**F**) ($n = 4$). *Significantly different from control, $^{*}P < 0.05$, $^{**}P < 0.01$, $^{***}P < 0.001$. $^{\#}$Significantly different from LPS group, $^{\#}P < 0.05$, $^{\#\#\#}P < 0.001$.

cytoplasmic lipid droplets colocalized with lysosomes, and their numbers were notably increased in LPS-stimulated HMGECs (Figs. 7A, 7B). In addition, incubation of HMGECs with LPS resulted in a significant increase in the number of LC3-labeled autophagosomes, indicating autophagy activation during LPS-stimulated lipogenesis (Figs. 7C, 7D). MLT supplementation yielded fewer cytoplasmic lysosomes and reduced LC3B-II staining (both $P < 0.01$). Additionally, MLT ameliorated the expression of Beclin 1 (fold change: 1.6 vs. 1.2, $P < 0.01$, Figs. 7E, 7F) and LC3B-II (fold change: 2.2 vs. 1.6, $P < 0.001$, Fig. 7G) in LPS-induced HMGECs, suggesting that MLT attenuated autophagy activation in LPS-stimulated HMGECs.

Pretreatment With MLT Inhibited Both the MAPK and NF-κB Pathways

To determine whether the MAPK/NF-κB pathway, which is the principal downstream target of TLR4/MyD88 signaling,[36] is involved in the protective effects of MLT on LPS-stimulated HMGECs, we further examined the expression of MAPK/NF-κB components by Western blotting. LPS significantly upregulated all of these pathway constituents, and the ratios of phosphorylated ERK, JNK, p38 MAPK, and p65 NF-κB to total ERK, JNK, p38 MAPK, and p65 NF-κB were increased in HMGECs after stimulation with LPS. Pretreatment with MLT markedly decreased the phosphorylation of ERK, JNK, p38 MAPK, and p65 NF-κB, whereas the total protein levels were not influenced by MLT (Fig. 8, all $P < 0.05$).

Discussion

In the present study, we investigated the inhibitory effect of MLT on the proinflammatory cytokine response and lipogenesis in LPS-stimulated HMGECs and explored the molecular mechanism. We described the expression pattern of TLR4 and MLT receptors in human MG acini and HMGECs. Our results demonstrated that pretreatment with MLT significantly inhibited TLR4/MyD88 signaling, the levels of proinflammatory (IL-1β, IL-6, IL-8, TNF-α) and matrix-degrading cytokines (MMP-3 and MMP-9), and lipogenesis in LPS-stimulated HMGECs. Furthermore, apoptosis and autophagy, as well as the MAPK/NF-κB pathway, were significantly activated during lipogenesis in LPS-stimulated HMGECs. MLT supplementation significantly attenuated LPS-induced apoptosis and autophagy by suppressing ERK, JNK, p38 MAPK, and p65 NF-κB phosphorylation.

TLRs are transmembrane proteins that have been widely identified in the mucosal system of the ocular surface, such as the cornea, limbus, and conjunctiva.[37] TLR recognizes oxidants and microbial proteins to initiate the innate immune response activating multiple steps in inflammatory reactions in the ocular surface.[38,39] Although Chen et al.[40] reported that LPS upregulated gene ontologies in the TLR signaling pathway in HMGECs, the expression pattern of TLR in MG tissue is less well understood. In our study, we found that TLR4 exhibited a similar expression pattern in MG as in SG[41,42] and was strongly expressed in human MG acini and distributed diffusely in the cytoplasm of HMGECs, suggesting the immunologic activity of human MG.

Investigative Ophthalmology & Visual Science

Downloaded from hwmaint.iovs.org on 04/19/2024

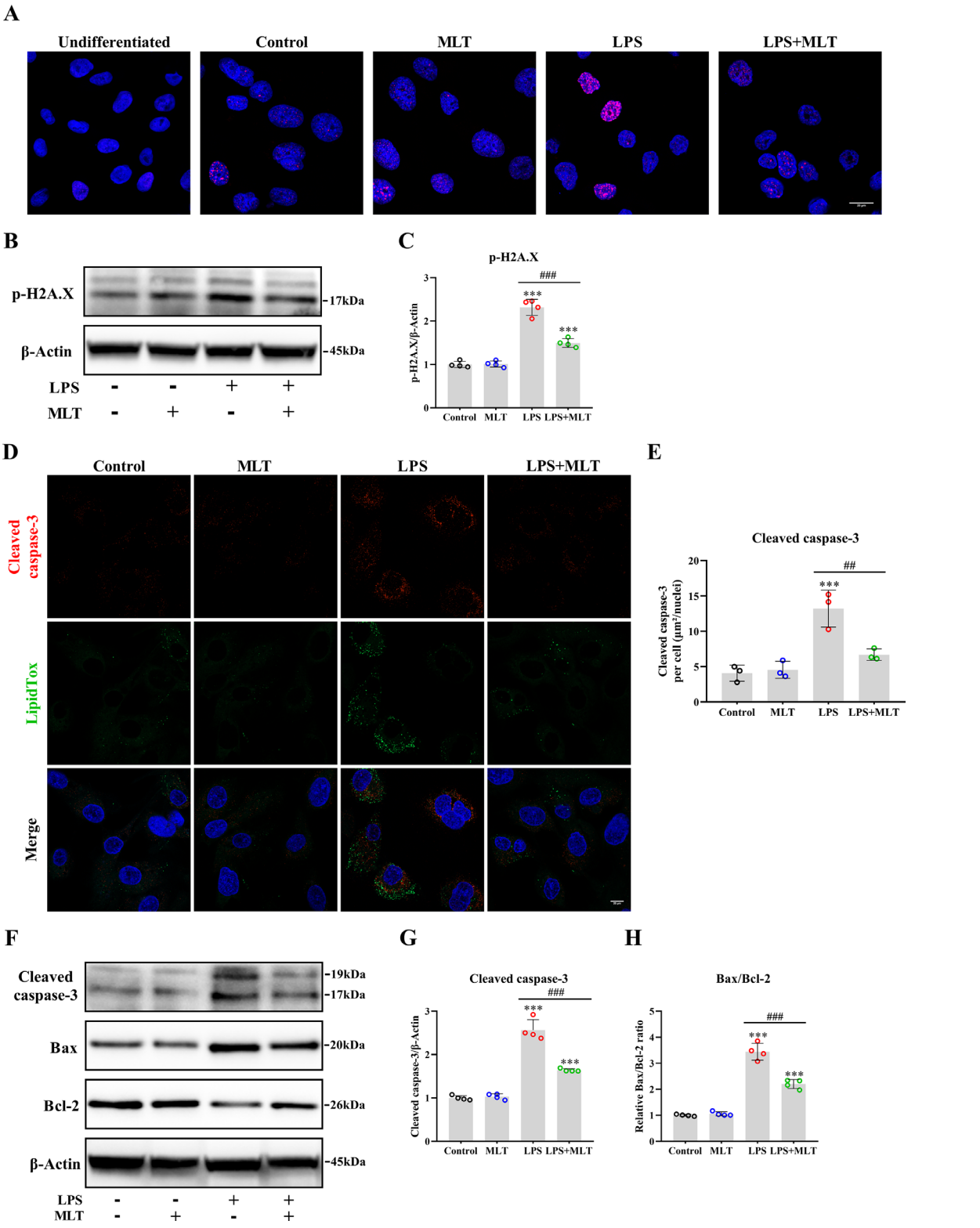

Figure 6. MLT attenuated apoptosis in LPS-stimulated HMGECs. The HMGECs were treated with MLT for 48 hours followed by LPS for 24 hours. The undifferentiated group was not treated with the differentiated medium. (**A**) Images of phospho-histone H2A.X foci in HMGECs depicted by immunofluorescence staining. *Scale bar*: 20 μm. (**B**) Representative protein bands of phospho-histone H2A.X. (**C**) Quantitative intensity of phospho-histone H2A.X ($n = 4$). (**D**) Images of cleaved caspase 3 in HMGECs obtained by immunofluorescence staining. (**E**) Fluorescence intensity quantitation of cleaved caspase 3 ($n = 3$). *Scale bar*: 20 μm. (**F**) Representative protein bands of cleaved caspase 3, Bax, and Bcl-2. (**G**, **H**) Quantitative intensity of cleaved caspase 3 (**G**) and Bax/Bcl-2 (**H**) ($n = 4$). ***Significantly different from control, ***$P < 0.001$. ##Significantly different from LPS group, ##$P < 0.01$, ###$P < 0.001$.

Investigative Ophthalmology & Visual Science

Downloaded from hwmaint.iovs.org on 04/19/2024

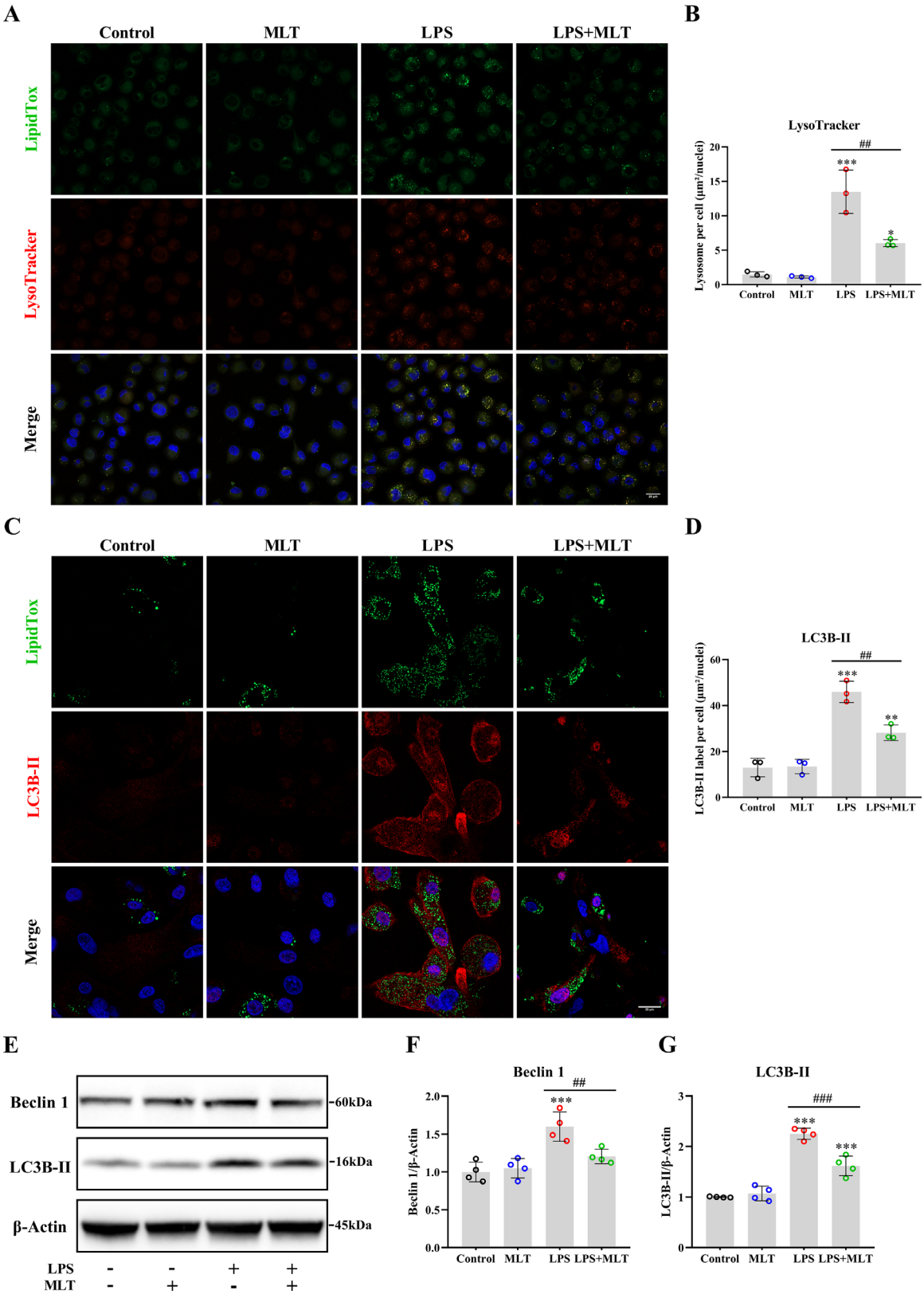

Figure 7. MLT attenuated autophagy in LPS-stimulated HMGECs. The HMGECs were treated with MLT for 48 hours followed by LPS for 24 hours. (**A**) Images of lysosome in HMGECs obtained by LysoTracker staining. *Scale bar*: 20 µm. (**B**) Fluorescence intensity quantitation of lysosome ($n = 3$). (**C**) Images of LC3B-II in HMGECs obtained by immunofluorescence staining. *Scale bar*: 20 µm. (**D**) Fluorescence intensity quantitation of LC3B-II ($n = 3$). (**E**) Representative protein bands of Beclin 1 and LC3B-II. (**F**, **G**) Quantitative intensity of Beclin 1 (**F**) and LC3B-II (**G**) ($n = 4$). *Significantly different from control, $^{*}P < 0.05$, $^{**}P < 0.01$, $^{***}P < 0.001$. $^{\#\#}$Significantly different from LPS group, $^{\#\#}P < 0.01$, $^{\#\#\#}P < 0.001$.

Investigative Ophthalmology & Visual Science

Downloaded from hwmaint.iovs.org on 04/19/2024

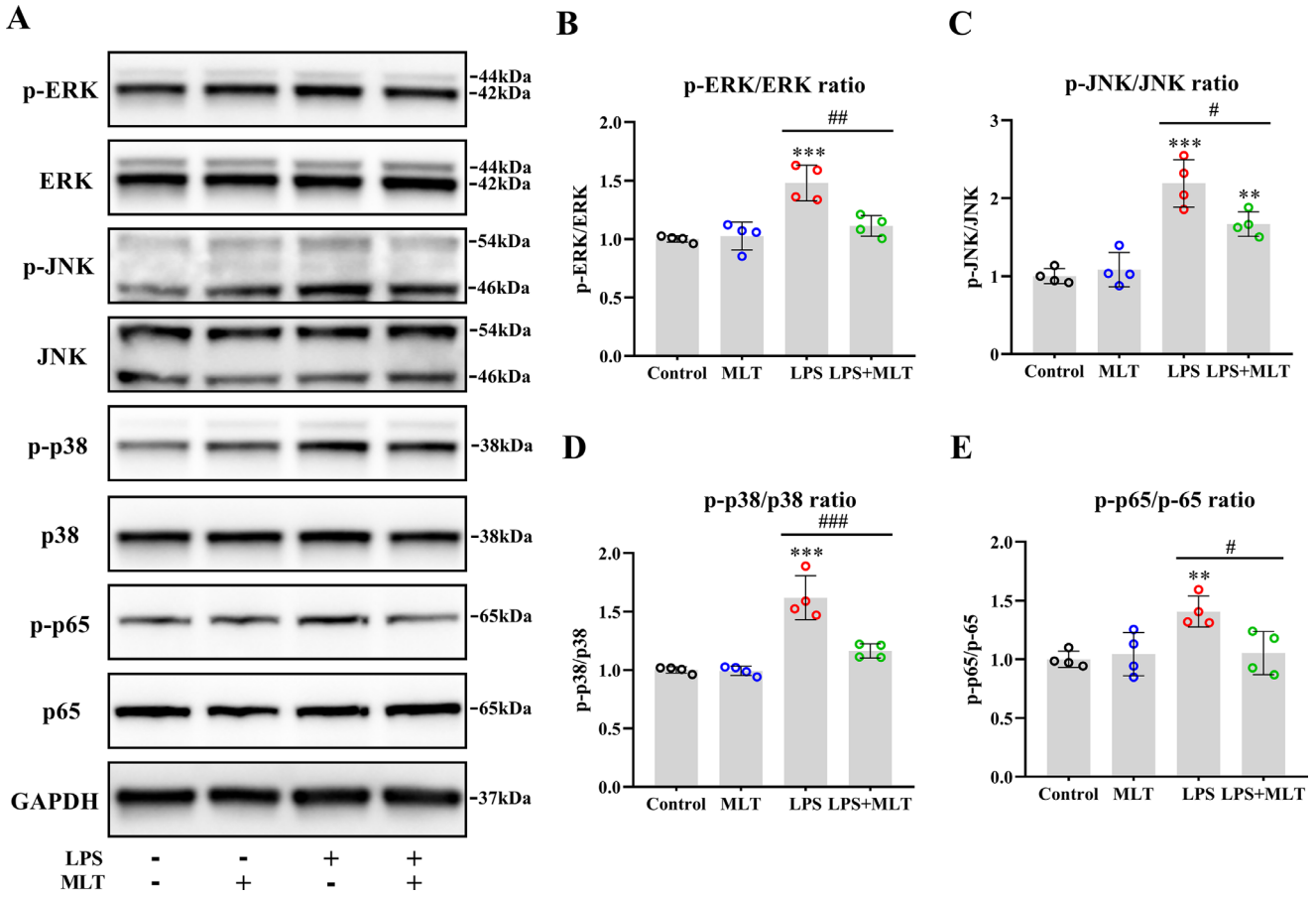

Figure 8. MLT suppressed the activation of MAPK and NF-κB pathway in LPS-stimulated HMGECs. The HMGECs were treated with MLT for 48 hours followed by LPS for 1 hour. (**A**) Representative protein bands of p-ERK, ERK, p-JNK, JNK p-p38 MAPK, p38 MAPK, p-p65 NF-κB, and p65 NF-κB. (**B–E**) Quantitative intensity of p-ERK/ERK (**B**), p-JNK/JNK (**C**), p-p38/p38 MAPK (**D**), and p-p65/p65 NF-κB (**E**). $n = 4$. *Significantly different from control, $^{**}P < 0.01$, $^{***}P < 0.001$. #Significantly different from LPS group, $^{\#}P < 0.05$, $^{\#\#}P < 0.01$, $^{\#\#\#}P < 0.001$.

Considering that patients with MGD showed an imbalance in the ocular surface microbiome, the culture-positive rate of bacteria in MG secretions from MGD patients was much higher than that in healthy individuals, indicating the pathogenicity of the bacterial toxins on MGD needs to be considered.[43] Additionally, for the first time, our results revealed that the MLT receptors MT_1 and MT_2 were both strongly expressed in human MG acini and HMGECs, indicating the regulatory potential of MLT on MG. Notably, the two MLT receptors have different expression patterns in HMGECs; MT_1 is mostly expressed in the cell membrane, while MT_2 is mainly expressed in the cell cytoplasm.

Elevated levels of proinflammatory cytokines (IL-1β, IL-6, IL-8, and TNF-α) and matrix-degrading cytokines (MMP-3 and MMP-9) within the MG may be involved in the development of MGD.[11–14,44] Stimulation with proinflammatory cytokine IL-1β induced hyperkeratinization in MG ducts.[13] In mice with inflammatory MGD, there was obvious inflammatory cell accumulation in the microenvironment surrounding the MG, and the expression of IL-1β, IL-6, TNF-α, MMP-3, and MMP-9 in the MG was significantly upregulated.[11] Our results also showed that LPS activated TLR4/MyD88 signaling to upregulate the levels of cytokines in HMGECs, including IL-1β, IL-6, IL-8, TNF-α, MMP-3, and MMP-9. Mahajan et al.[9] recently reported that neutrophil infiltration in the MG lumen could contribute to inflammatory obstruction in MGD, suggesting that MG occlusion requires the influx of neutrophils. Considering that IL-1β, IL-6, IL-8, TNF-α, and MMP-3/9 are important neutrophil chemoattractants that orchestrate migration and infiltration,[45–49] the proinflammatory cytokine response of meibocytes may facilitate neutrophil chemoattraction and activation to induce MG obstruction.

Previous studies have demonstrated that proinflammatory stimuli induce differentiation and lipogenesis disorders in lipogenic cells in several diseases such as obesity and acne.[15,50] Herein, we also observed that the TLR4-mediated proinflammatory cytokine responses play an essential role in the imbalance in lipogenesis and differentiation in HMGECs, which may explain the abnormalities of meibum lipids of MGD.[11] TLR4-mediated proinflammatory responses induced lipogenesis in HMGECs, whereas prophylactic supplementation with MLT showed a considerable anti-inflammatory effect that markedly inhibited the proinflammatory cytokine responses and downregulated the protein levels of ADFP, SREBP-1, and ELOVL4, as well as attenuated lipogenesis and differentiation in LPS-stimulated HMGECs. ADFP is expressed early in adipocytes and acts as a marker of meibocyte differentiation.[51] SREBP-1 and ELOVL4 are responsible for the synthesis and metabolism of very long-chain fatty acids and cholesterol in meibum lipids, respectively.[52,53] Considering that these proteins play roles in the metabolism

Investigative Ophthalmology & Visual Science

Downloaded from hwmaint.iovs.org on 04/19/2024

of meibum lipids, the inhibitory effects of MLT on LPS-induced inflammatory lipogenesis could have clinical implications in the treatment of MGD.

Our data demonstrated that the level of phospho-histone H2A.X increased with HMGEC differentiation, indicating active DNA damage and repair, which was consistent with the theory that the terminal differentiation of MG cells involves programmed cell death.[1] The terminal differentiation of MG cells requires the apoptosis-induced DNA strand break in the nucleus and autophagy-mediated degradation of the nucleus and cytoplasmic organelles to disintegrate and release cellular contents.[1,35] We found that proinflammatory stress could facilitate lipogenesis and accelerate the terminal fate of HMGECs related to the overactivation of apoptosis and autophagy, which may play a pathologic role in lipid abnormalities and acini dropout in MGD. Consistent with our findings, Guo et al.[10] recently reported that there was a prominent proinflammatory cytokine response, lipid accumulation, glandular dropout, and cell death in rats with MGD induced by hyperglycemia. Kim et al.[54] also suggested that autophagy was initiated and mediated for cellular disintegration during the late differentiation of HMGECs. MLT supplementation could regulate the differentiation of several cell types by mediating apoptosis and autophagy.[55,56] Consistently, we observed the therapeutic effects of MLT, which alleviated the mitochondria-dependent apoptotic pathway characterized by perturbations in the Bax/Bcl-2 rheostat and inhibition of the executioner caspase 3. In addition, MLT also suppressed the expression of Beclin 1 and LC3B-II to inhibit autophagy during lipogenesis in LPS-stimulated HMGECs.

We found that MLT significantly suppressed the phosphorylation of MAPK/NF-κB components during LPS-induced lipogenesis in HMGECs. The MAPK/NF-κB pathway can induce apoptosis and autophagy in several adipogenic cells in response to extracellular proinflammatory stimuli.[15,16,57] In mice fed a high-fat diet, the activation of MAPK/NF-κB regulates the Bax/Bcl-2 proportions to change the mitochondrial membrane potential, leading to the activation of caspase 3 and the induction of apoptosis and hepatic steatosis.[58] In response to stress signals of advanced glycation end products, MAPK/NF-κB also induces the dissociation of Beclin 1 and activates LC3 to mediate lipogenesis-related autophagy in HepG2 cells.[57] Based on these findings, we surmise that MLT may regulate the proinflammatory cytokine response, lipogenesis, and related cell death by modulating the MAPK/NF-κB pathway in HMGECs.

Inconsistent with previous studies, we found that MLT showed no influence on lipid synthesis or differentiation in HMGECs, which could be explained by the diversity of cell types and MLT concentrations used in different studies. González et al.[31] showed that MLT induced the differentiation and adipogenesis of 3T3-L1 adipocytes by activating the PPARγ pathway, while Basoli et al.[32] revealed that MLT inhibited obesity in adipose-derived stem cells by suppressing the expression of adipogenesis orchestrating genes. Noticeably, the concentrations of MLT used in these studies were both over 1 mM, which was much higher than the effective concentration that has been shown to play an anti-inflammatory role and the levels in human tears (<100 µM).[27,59] In addition, in our study, a higher concentration of MLT significantly decreased the viability of HMGECs in vitro. In summary, MLT in tears may mainly exert anti-inflammatory effects on the MG to prevent lipogenesis disorders, and MLT pretreatment may be a suitable strategy to prevent MGD.

There are some limitations in this study. First, our MG samples were collected from eyelid surgery, and few ductal parts were obtained; therefore, the immunohistochemical staining results mainly depicted the related characteristics of MG acini. Second, although MT_1 and MT_2 were both expressed in the MG, they showed different structures, affinities, and therapeutic potentials,[60] so determining which receptor mediates the protective effects of MLT on the MG requires further study.

In summary, this study identified the immunologic activity and MLT receptors in human meibocytes. Our data provide a supplement to the pathologic mechanism of MGD and show that proinflammatory stimuli can increase lipogenesis, apoptosis, and autophagy in meibocytes, which may explain the lipid abnormalities and glandular dropout in inflammatory MGD. The physiologic concentration of MLT could prevent a series of pathologic reactions in meibocytes caused by proinflammatory stimuli. Prophylactic supplementation with MLT markedly attenuated lipogenesis, apoptosis, and autophagy in LPS-stimulated HMGECs by suppressing the TLR4-mediated MAPK/NF-κB pathway, suggesting that MLT could be a promising therapy for MGD.

Acknowledgments

The authors thank Sullivan (Schepens Eye Research Institute) for kindly providing the HMGECs.

Supported by the National Natural Science Foundation of China (81770892, 82070922), the Science Foundation of Guangdong Province (2019A1515012012), and the High-level Hospital Foundation (303020101). The sponsors or funding organizations have no role in the design or implementation of this study; collection, management, analysis, and interpretation of the data; and preparation, review, or approval of the manuscript.

Disclosure: **R. Liu**, None; **J. Li**, None; **Y. Xu**, None; **Z. Chen**, None; **H. Ye**, None; **J. Tang**, None; **L. Wei**, None; **L. Liang**, None

References

1. Knop E, Knop N, Millar T, Obata H, Sullivan DA. The international workshop on meibomian gland dysfunction: report of the Subcommittee on Anatomy, Physiology, and Pathophysiology of the Meibomian Gland. *Invest Ophthalmol Vis Sci*. 2011;52:1938–1978.
2. Obata H. Anatomy and histopathology of human meibomian gland. *Cornea*. 2002;21:S70–S74.
3. Liu S, Hatton MP, Khandelwal P, Sullivan DA. Culture, immortalization, and characterization of human meibomian gland epithelial cells. *Invest Ophthalmol Vis Sci*. 2010;51:3993–4005.
4. Chhadva P, Goldhardt R, Galor A. Meibomian gland disease: the role of gland dysfunction in dry eye disease. *Ophthalmology*. 2017;124:S20–S26.
5. Hassanzadeh S, Varmaghani M, Zarei-Ghanavati S, Heravian Shandiz J, Azimi Khorasani A. Global prevalence of meibomian gland dysfunction: a systematic review and meta-analysis. *Ocul Immunol Inflamm*. 2021;29:66–75.
6. Eom Y, Lee JS, Kang SY, Kim HM, Song JS. Correlation between quantitative measurements of tear film lipid layer thickness and meibomian gland loss in patients with obstructive meibomian gland dysfunction and normal controls. *Am J Ophthalmol*. 2013;155:1104–1110.e1102.

Downloaded from hwmaint.iovs.org on 04/19/2024

7. Bron AJ, de Paiva CS, Chauhan SK, et al. TFOS DEWS II pathophysiology report. *Ocular Surface*. 2017;15:438–510.
8. Reyes NJ, Yu C, Mathew R, et al. Neutrophils cause obstruction of eyelid sebaceous glands in inflammatory eye disease in mice. *Sci Transl Med*. 2018;10:eaas9164.
9. Mahajan A, Hasíková L, Hampel U, et al. Aggregated neutrophil extracellular traps occlude meibomian glands during ocular surface inflammation. *Ocular Surface*. 2021;20:1–12.
10. Guo Y, Zhang H, Zhao Z, et al. Hyperglycemia induces meibomian gland dysfunction. *Invest Ophthalmol Vis Sci*. 2022;63:30.
11. Bu J, Zhang M, Wu Y, et al. High-fat diet induces inflammation of meibomian gland. *Invest Ophthalmol Vis Sci*. 2021;62:13–13.
12. Bu J, Wu Y, Cai X, et al. Hyperlipidemia induces meibomian gland dysfunction. *Ocular Surface*. 2019;17:777–786.
13. Xu KK, Huang YK, Liu X, Zhang MC, Xie HT. Organotypic culture of mouse meibomian gland: a novel model to study meibomian gland dysfunction in vitro. *Invest Ophthalmol Vis Sci*. 2020;61:30.
14. Chen H, Gao H, Xie H-T, Liu S-T, Huang Y-K, Zhang M-C. Hyperkeratinization and proinflammatory cytokine expression in meibomian glands induced by *Staphylococcus aureus*. *Invest Ophthalmol Vis Sci*. 2021;62:11.
15. Lee SE, Kim JM, Jeong SK, Choi EH, Zouboulis CC, Lee SH. Expression of protease-activated receptor-2 in SZ95 sebocytes and its role in sebaceous lipogenesis, inflammation, and innate immunity. *J Invest Dermatol*. 2015;135:2219–2227.
16. Choi CW, Kim Y, Kim JE, et al. Enhancement of lipid content and inflammatory cytokine secretion in SZ95 sebocytes by palmitic acid suggests a potential link between free fatty acids and acne aggravation. *Exp Dermatol*. 2019;28:207–210.
17. Stehle JH, Saade A, Rawashdeh O, et al. A survey of molecular details in the human pineal gland in the light of phylogeny, structure, function and chronobiological diseases. *J Pineal Res*. 2011;51:17–43.
18. Cipolla-Neto J, Amaral FGD. Melatonin as a hormone: new physiological and clinical insights. *Endocrine Rev*. 2018;39:990–1028.
19. Stauch B, Johansson LC, McCorvy JD, et al. Structural basis of ligand recognition at the human MT(1) melatonin receptor. *Nature*. 2019;569:284–288.
20. Johansson LC, Stauch B, McCorvy JD, et al. XFEL structures of the human MT(2) melatonin receptor reveal the basis of subtype selectivity. *Nature*. 2019;569:289–292.
21. Meyer P, Pache M, Loeffler KU, et al. Melatonin MT-1-receptor immunoreactivity in the human eye. *Br J Ophthalmol*. 2002;86:1053–1057.
22. Reyes-Resina I, Awad Alkozi H, Del Ser-Badia A, et al. Expression of melatonin and dopamine D(3) receptor heteromers in eye ciliary body epithelial cells and negative correlation with ocular hypertension. *Cells*. 2020;9(1):152.
23. Pang SF, Yu HS, Suen HC, Brown GM. Melatonin in the retina of rats: a diurnal rhythm. *J Endocrinol*. 1980;87:89–93.
24. Alkozi HA, Wang X, Perez de Lara MJ, Pintor J. Presence of melanopsin in human crystalline lens epithelial cells and its role in melatonin synthesis. *Exp Eye Res*. 2017;154:168–176.
25. Alkozi HA, Perez de Lara MJ, Pintor J. Melatonin synthesis in the human ciliary body triggered by TRPV4 activation: involvement of AANAT phosphorylation. *Exp Eye Res*. 2017;162:1–8.
26. Mhatre MC, van Jaarsveld AS, Reiter RJ. Melatonin in the lacrimal gland: first demonstration and experimental manipulation. *Biochem Biophys Res Commun*. 1988;153:1186–1192.
27. Carracedo G, Carpena C, Concepción P, et al. Presence of melatonin in human tears. *J Optom*. 2017;10:3–4.
28. Chiquet C, Claustrat B, Thuret G, Brun J, Cooper HM, Denis P. Melatonin concentrations in aqueous humor of glaucoma patients. *Am J Ophthalmol*. 2006;142:325–327.e321.
29. Del Sole MJ, Sande PH, Fernandez DC, Sarmiento MI, Aba MA, Rosenstein RE. Therapeutic benefit of melatonin in experimental feline uveitis. *J Pineal Res*. 2012;52:29–37.
30. Aranda ML, González Fleitas MF, De Laurentiis A, et al. Neuroprotective effect of melatonin in experimental optic neuritis in rats. *J Pineal Res*. 2016;60:360–372.
31. González A, Alvarez-García V, Martínez-Campa C, Alonso-González C, Cos S. Melatonin promotes differentiation of 3T3-L1 fibroblasts. *J Pineal Res*. 2012;52:12–20.
32. Basoli V, Santaniello S, Cruciani S, et al. Melatonin and vitamin D interfere with the adipogenic fate of adipose-derived stem cells. *Int J Mol Sci*. 2017;18(5):981.
33. Marangoz D, Oner C, Schicht M, et al. The effect of androgens on proinflammatory cytokine secretion from human ocular surface epithelial cells. *Ocul Immunol Inflamm*. 2021;29:546–554.
34. Wróbel A, Seltmann H, Fimmel S, et al. Differentiation and apoptosis in human immortalized sebocytes. *J Invest Dermatol*. 2003;120:175–181.
35. Liu Y, Kam WR, Ding J, Sullivan DA. One man's poison is another man's meat: using azithromycin-induced phospholipidosis to promote ocular surface health. *Toxicology*. 2014;320:1–5.
36. Fitzgerald KA, Palsson-McDermott EM, Bowie AG, et al. Mal (MyD88-adapter-like) is required for Toll-like receptor-4 signal transduction. *Nature*. 2001;413:78–83.
37. Lambiase A, Micera A, Sacchetti M, Mantelli F, Bonini S. Toll-like receptors in ocular surface diseases: overview and new findings. *Clin Sci*. 2011;120:441–450.
38. Kawai T, Akira S. TLR signaling. *Cell Death Differ*. 2006;13:816–825.
39. Galletti JG, de Paiva CS. The ocular surface immune system through the eyes of aging. *Ocular Surface*. 2021;20:139–162.
40. Chen D, Sahin A, Kam WR, Liu Y, Darabad RR, Sullivan DA. Influence of lipopolysaccharide on proinflammatory gene expression in human corneal, conjunctival and meibomian gland epithelial cells. *Ocular Surface*. 2018;16:382–389.
41. Zouboulis CC, Oeff MK, Hiroi N, Makrantonaki E, Bornstein SR. Involvement of pattern recognition receptors in the direct influence of bacterial components and standard antiacne compounds on human sebaceous gland cells. *Skin Pharmacol Physiol*. 2021;34:19–29.
42. Oeff MK, Seltmann H, Hiroi N, et al. Differential regulation of Toll-like receptor and CD14 pathways by retinoids and corticosteroids in human sebocytes. *Dermatology*. 2006;213:266.
43. Zhang SD, He JN, Niu TT, et al. Bacteriological profile of ocular surface flora in meibomian gland dysfunction. *Ocular Surface*. 2017;15:242–247.
44. Dong ZY, Ying M, Zheng J, Hu LJ, Xie JY, Ma Y. Evaluation of a rat meibomian gland dysfunction model induced by closure of meibomian gland orifices. *Int J Ophthalmol*. 2018;11:1077–1083.
45. Verri WA, Jr, Souto FO, Vieira SM, et al. IL-33 induces neutrophil migration in rheumatoid arthritis and is a target of anti-TNF therapy. *Ann Rheum Dis*. 2010;69:1697–1703.
46. Wright HL, Cross AL, Edwards SW, Moots RJ. Effects of IL-6 and IL-6 blockade on neutrophil function in vitro and in vivo. *Rheumatology*. 2014;53:1321–1331.
47. de Boer JH, Hack CE, Verhoeven AJ, et al. Chemoattractant and neutrophil degranulation activities related to interleukin-8 in vitreous fluid in uveitis and vitreoretinal disorders. *Invest Ophthalmol Vis Sci*. 1993;34:3376–3385.

Investigative Ophthalmology & Visual Science

Downloaded from hwmaint.iovs.org on 04/19/2024

48. Kruidenier L, MacDonald TT, Collins JE, Pender SL, Sanderson IR. Myofibroblast matrix metalloproteinases activate the neutrophil chemoattractant CXCL7 from intestinal epithelial cells. *Gastroenterology* .2006;130:127–136.
49. Stefanidakis M, Ruohtula T, Borregaard N, Gahmberg CG, Koivunen E. Intracellular and cell surface localization of a complex between alphaMbeta2 integrin and promatrix metalloproteinase-9 progelatinase in neutrophils. *J Immunol*. 2004;172:7060–7068.
50. Gong Z, Zhang X, Su K, et al. Deficiency in AIM2 induces inflammation and adipogenesis in white adipose tissue leading to obesity and insulin resistance. *Diabetologia*. 2019;62:2325–2339.
51. Kim SW, Xie Y, Nguyen PQ, et al. PPARγ regulates meibocyte differentiation and lipid synthesis of cultured human meibomian gland epithelial cells (hMGEC). *Ocular Surface*. 2018;16:463–469.
52. Liu Y, Ding J. The combined effect of azithromycin and insulin-like growth factor-1 on cultured human meibomian gland epithelial cells. *Invest Ophthalmol Vis Sci*. 2014;55:5596–5601.
53. Hopiavuori BR, Anderson RE, Agbaga MP. ELOVL4: very long-chain fatty acids serve an eclectic role in mammalian health and function. *Prog Retin Eye Res*. 2019;69:137–158.
54. Kim SW, Rho CR, Kim J, et al. Eicosapentaenoic acid (EPA) activates PPARγ signaling leading to cell cycle exit, lipid accumulation, and autophagy in human meibomian gland epithelial cells (hMGEC). *Ocular Surface*. 2020;18:427–437.
55. Xiao L, Lin J, Chen R, et al. Sustained release of melatonin from GelMA liposomes reduced osteoblast apoptosis and improved implant osseointegration in osteoporosis. *Oxid Med Cell Longev*. 2020;2020:6797154.
56. Li H, Zhang Y, Liu S, et al. Melatonin enhances proliferation and modulates differentiation of neural stem cells via autophagy in hyperglycemia. *Stem Cells*. 2019;37:504–515.
57. Sui X, Kong N, Ye L, et al. p38 and JNK MAPK pathways control the balance of apoptosis and autophagy in response to chemotherapeutic agents. *Cancer Lett*. 2014;344:174–179.
58. Sinha-Hikim I, Sinha-Hikim AP, Shen R, et al. A novel cystine based antioxidant attenuates oxidative stress and hepatic steatosis in diet-induced obese mice. *Exp Mol Pathol*. 2011;91:419–428.
59. Chang CC, Tien CH, Lee EJ, et al. Melatonin inhibits matrix metalloproteinase-9 (MMP-9) activation in the lipopolysaccharide (LPS)-stimulated RAW 264.7 and BV2 cells and a mouse model of meningitis. *J Pineal Res*. 2012;53:188–197.
60. Alarma-Estrany P, Pintor J. Melatonin receptors in the eye: location, second messengers and role in ocular physiology. *Pharmacol Ther*. 2007;113:507–522.

Investigative Ophthalmology & Visual Science

Downloaded from hwmaint.iovs.org on 04/19/2024